Infrasound and Low-Frequency Noise from Wind Turbines

Conference Paper · July 2015

DOI: 10.1007/978-3-662-48868-3_1

3 authors:

Colin H Hansen
University of Adelaide

Branko Zajamsek
Flinders University

Kristy Hansen
Flinders University

Infrasound and low-frequency noise from wind turbines

Colin Hansen, Branko Zajamšek and Kristy Hansen

Abstract Infrasound, low-frequency noise (ILFN) and amplitude modulation of the noise are known to disturb some residents living near wind farms. However, the mechanisms responsible for ILFN and amplitude modulation are not well understood. In an attempt to shed some light on these mechanisms, acoustic measurements were taken in the close vicinity of a wind farm, at residences located two or more kilometres from the nearest turbine in a wind farm and in an anechoic chamber using a scale-model, electrically-driven, wind turbine. The measured spectra reveal distinct peaks at the blade-pass frequency and harmonics, and the characteristics of these peaks are remarkably similar for field and laboratory measurements, indicating that the zero mean flow simulation is a good representation of an actual wind turbine. Near field acoustic holography measurements on the scale-model turbine confirm that tonal components at the blade-pass frequency and harmonics are generated as a result of blade-tower interaction, suggesting that it is likely to be an important mechanism of infrasound generation for industrial wind turbines. Inaccuracies in the assumed location of noise sources on a wind turbine affect the accuracy of community noise predictions. This is because the source height affects the distance from the turbine beyond which sound rays arrive at the receiver having been reflected from the ground more than once, thus reducing the attenuation with distance from the turbine.

1 Introduction

One of the drawbacks of wind energy is that turbines generate sufficient noise to result in adverse reactions from some nearby residents. The noise that causes problems is infrasound and low-frequency noise (ILFN) and the associated noise levels are highly variable as a function of time, due to meteorological factors, blade loading

Colin Hansen
The University of Adelaide, North Terrace, Adelaide, South Australia, 5000
e-mail: colin.hansen@adelaide.edu.au

Branko Zajamšek
University of New South Wales, Kensington, Sydney, NSW, 2052
e-mail: b.zajamsek@student.unsw.edu.au

Kristy Hansen
Flinders University, Bedford Park, Adelaide, South Australia, 5042
e-mail: kristy.hansen@flinders.edu.au

variations, directivity variations as the turbine blades rotate, and interaction between the sound from two or more turbines. These characteristics make wind turbine noise more annoying at comparable levels than other sources such as industrial and transportation noise. Also, low frequency noise and infrasound are less attenuated over large propagation distances and can penetrate buildings more readily than mid- to high-frequency noise.

In the future, the size of wind turbines is expected to increase since larger turbines are more efficient energy generators. Unfortunately, this will lead to an increase in the thrust force acting on the blades as well as an increase in the infrasound and low-frequency noise due to higher hub heights, which introduce larger variations in blade loading during a revolution. Larger wind turbines also rotate more slowly due to limitations in the allowable blade-tip velocity and therefore mechanical noise is expected to decrease in frequency. A downward shift of the noise spectrum by approximately one-third of an octave has already been observed in the transition from small to large wind turbines (Møller and Pedersen, 2011). If infrasound and low frequency noise are to be reduced, it is important that the corresponding noise generation and propagation mechanisms are well understood.

2 Effect of wind turbine noise on people

Many residents who live in close proximity to wind farms report annoyance and sleep disturbance, even when the measured noise levels are relatively low. One reason for this is that wind turbines are often located in rural areas where background noise levels are very low, particularly at night time. The contrast between ambient noise and noise due to wind farm operation is also exacerbated during the evening and night-time due to stable atmospheric conditions (Van den Berg, 2004). During these conditions, the wind turbines continue to operate, while the wind speed at residences is negligible, so corresponding background noise levels are often well below 20 dBA.

Stable atmospheric conditions are also characterised by high wind shear, which has been suggested as a major factor responsible for the amplitude modulation of wind turbine noise (RenewableUK, 2013). Residents living in the vicinity of wind farms describe the associated noise as “thumping” (Van den Berg, 2004) or “rumbling” (Hansen et al., 2014) in character, indicating the presence of low frequency, time varying noise. The difference between the audibility threshold and perceived loudness is small when the noise is dominated by low-frequencies (Møller and Pedersen, 2004) and therefore if a low-frequency noise is amplitude modulated as well as being above the normal hearing threshold, it is likely to be annoying to many people.

Some people living near wind farms also report symptoms of motion sickness, including ear pressure, headache, nausea, dizziness and vertigo. It is possible that these symptoms are related to exposure to infrasound, which is primarily generated as a result of blade-tower interaction. The amplitude of vertical motion in the 2 Hz to 4 Hz range required to produce seasickness in sensitive individuals corresponds to an atmospheric pressure variation that is similar to the levels of acoustic pressure variation experienced by people living in the vicinity of wind farms (Dooley, 2013). The regular, periodic nature of these variations, or the symmetry of the maximum and minimum values compared to the mean, may explain why similar levels of random environmental infrasound do not result in motion sickness symptoms in sensitive individuals. Another explanation for adverse health symptoms reported by people living near wind farms is that infrasound stimulates the outer hair cells of the human ear at levels below the audibility threshold (Salt and Lichtenhan, 2014). This results in information transfer via pathways that do not involve conscious hearing, which may lead to sensations of fullness, pressure or tinnitus, or lead to no sensation at all. Salt′s work is by no means generally accepted and the subject of infrasound is still surrounded by controversy and ongoing debate about its significance. One or more of the above mentioned symptoms can also be attributed to excessive exposure to low frequency noise.

3 Infrasound and low-frequency noise generating mechanisms

Wind turbines generate infrasound and low-frequency sound, as well as mid-and high-frequency sound. However, as low-frequency sound and infrasound are not attenuated by atmospheric absorption or reflection from the ground, they dominate the noise spectrum at residences more than one or two kilometres from the wind farm. These sounds are either aeroacoustic or mechanical in origin and can be either tonal or broadband in nature, depending on the generation mechanism. Aerodynamic infrasound and low-frequency noise originate as a result of changes in the aerodynamic force acting on the blades as they rotate. This can be caused by wind shear, atmospheric turbulence, cross-wind conditions, or interaction with the disturbed flow between the blade and tower as the blade passes the tower. The disturbed flow is a result of the flow streamlines having to deviate to negotiate the tower obstacle. It has been shown analytically that this phenomenon, illustrated in Fig. 1, is responsible for variations in the blade loading and hence generation of tonal components at the blade-pass frequency and harmonics (Doolan et al., 2012). In Fig. 1, it can be seen that the potential flow over the support tower creates a region of reduced velocity in front of the support tower. When the blade passes through that region, the angle of attack varies which changes the lift force and subsequently produces sound.

Interaction between inflow turbulence and the rotating turbine blades also leads to aerodynamic loading fluctuations, which are responsible for the generation of low frequency, broadband noise. The level of inflow turbulence, and hence noise generation, varies with atmospheric conditions and also with the locations of turbines relative to the wake of other turbines. The resulting far field noise from this interaction is strongly dependent on the inflow turbulence spectrum. Large eddies in the inflow cause a change in the aerodynamic force over the whole blade surface and

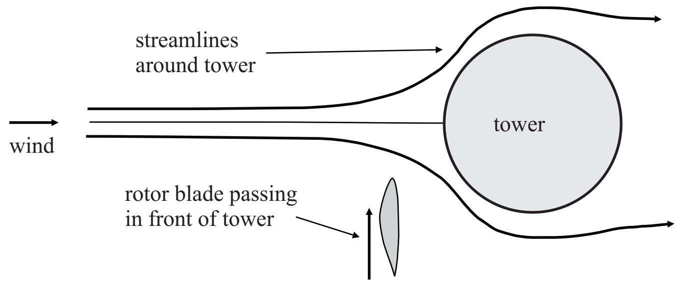

Fig. 1 Blade-tower interaction

consequently noise radiation has a dipole directivity pattern and the peak radiating frequency is low, typically below 20 Hz for a modern turbine (Doolan et al., 2012).

A general theory, explaining sound radiation due to unsteady blade loading was first proposed by (Tyler and Sofrin, 1962) for the case of turbo-machinery and was later expanded to an open rotor via the concept of pressure modes (Wright, 1976). More recently, this theory has been applied to wind turbines by (Dooley and Metelka, 2014). According to the theory, any rotor can be thought of as a system of rotating forces whose magnitude varies with rotor azimuthal position. These rotating forces can be simulated by a point source on the blade at a location, r_e, which is usually 0.8 times the blade span from the centre of the rotor plane. At any instant in time, these pressure variations are in-phase at each blade location, but they are not sinusoidal and thus can be described in terms of harmonics of the blade pass frequency, which rotate with the blade — hence their name, ”spinning modes”. The mode order indicates the number of 2π changes during one complete blade revolution.

Each pressure harmonic radiates noise in all directions, but the radiation to the side of the rotor is slightly greater. The tonal peaks in the radiated noise spectrum are broadened a little by the Doppler shift as a result of the motion of the blades. The broadening is dependent on the observer location and increases as the observer moves from on-axis to the side of the rotor plane.

When a rotating wind turbine blade passes the tower, the blade experiences a loading excursion that adds to the other pressure variations and increases the sound radiation in the directions normal to the rotor plane (see Fig. 2). Although the blade experiences the change in loading across the whole span, it can be simulated by an equivalent point loading at an effective radius, r_e. The sinusoidal signal at the top of the figure represents both the sound pressure variation as a function of time for a specified location as well as the sound pressure distribution around the circle containing the equivalent point sources at any instant in time. The sound field at an arbitrary observer is a function of the path difference x_1 and x_2 (see Fig. 2), and also linear phase variations around the spinning mode at p_1 and p_2. It is thus the modal phase and path difference that define the frequencies at which constructive and destructive interference occur at any particular location. This process produces characteristic interference lobes that radiate in specific directions, and which appear at higher blade-pass frequency harmonics.

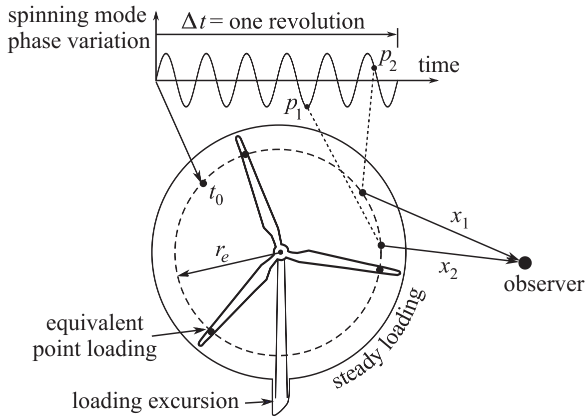

Fig. 2 Principle of spinning modes. The dashed line represents the effective radius of the equivalent point source and the solid line indicates the blade loading, showing a step excursion as a result of blade tower interaction

Loading unsteadiness caused by turbulent inflow is random in nature and is highly influenced by meteorological conditions, which affect the level of atmospheric turbulence as well as the characteristics of the wake generated by upstream turbines. Time-varying noise characteristics at the receiver can also be caused by constructive/destructive reinforcement of sound waves arriving at a residence from two or more wind turbines. The regions in which constructive/destructive interference occur are defined by the relative phase of the incoming sound waves, which varies with wind direction and blade rotation rate, leading to a time dependent amplitude variation of sound at any given location. This phenomenon is accentuated in stable atmospheric conditions which have low associated atmospheric turbulence, resulting in different turbines rotating at more similar speeds with reduced fluctuations (Van den Berg, 2005).

In addition to the random amplitude variations discussed above, periodic variations in the loudness (or amplitude modulation) of wind turbine noise also occur, with the frequency of variation generally equal to the rate at which blades pass the tower. In cases where local stall occurs, the trailing edge noise spectra shifts to lower frequencies and the resulting time-varying noise has been described as “thumping” (RenewableUK, 2013). In contrast to attached flow trailing edge noise, which shows most significant amplitude modulation in the crosswind direction at large distances (Oerlemans and Schepers, 2009), amplitude modulation associated with stall noise is highest in the upstream and downstream directions (RenewableUK, 2013).

Another noise source that is subject to amplitude modulation is gearbox noise. This can occur when the planetary gear mesh noise is amplitude modulated by the blade/planet-pass frequency and this phenomenon appears to be responsible for the “rumbling” noise that has been measured in the vicinity of the Waterloo wind farm in South Australia (Hansen et al., 2014).

4 Infrasound and low frequency noise propagation

In general, sound spreads spherically from a given source, resulting in an attenuation rate of 6 dB/doubling of distance. However, in the downwind direction, the wind speed gradient causes the sound waves to bend towards the ground, reducing the attenuation of noise in the downwind direction. Vertical temperature gradients also give rise to sound speed gradients, but the effect of the wind speed gradient is generally dominant in the propagation of sound from wind turbines. The effect of a downward refracting atmosphere is that beyond a certain distance, more than one ground reflected ray will arrive at the receiver. The first ground reflected ray will have been reflected from the ground once, the second ground reflected ray will have been reflected from the ground twice, etc.

The distance from the sound source at which sound will begin to attenuate at a rate less than 6 dB per doubling of distance is a function of the source height as well as the strength of the atmospheric sonic velocity gradient (and the consequent strength of the downward refraction), as this determines the distance from the source at which the receiver will experience the arrival of more than one ground reflected wave. The effect only occurs at low-frequencies for which losses due to ground reflection and atmospheric absorption are negligible. The path length of reflected sound rays increases as the number of reflections increase and so the amplitude of the sound pressure (relative to the direct, non-reflected ray) arriving at the receiver from each reflected ray decreases as the number of reflections increases, until after a certain number of reflections, a particular ray is no longer an important contributor to the sound pressure level at the receiver. It has been shown that the sum of all reflected rays results in a decay of the sound field of approximately 3 dB per doubling of distance (Willshire Jr and Zorumski, 1987), which is why it is often referred to as "cylindrical spreading". Of course there is a gradual transition over both decreasing frequency and increasing distance from the source, during which the decay rate changes from 6 dB to 3 dB per doubling of distance.

5 Experimental measurements of blade-tower interaction

To develop an understanding of how blade-tower interaction contributes to wind turbine infrasound and low-frequency noise generation, experimental work was undertaken in the anechoic chamber at the University of Adelaide using the scale-model wind turbine shown in Fig. 3a. The anechoic chamber has dimensions of $4.79 \times 3.9 \times 3.94$ m. The blades on the wind turbine model had a symmetrical airfoil shape, they were mounted at 0° angle of attack and they were driven by an electric motor in conditions of zero net flow. Although this experimental configuration does not replicate the effect of the reduced velocity field in-front of a turbine tower, which is the major source of unsteady aerodynamic loading, the blade-tower interaction is still adequately re-created via the interaction of the support tower with the potential velocity field surrounding the blade. The 0° angle of attack is ideal for studying

BTI as the resulting noise spectrum is not affected by noise generated by thrust and torque loading. However, for zero angle of attack symmetrical blades, the pressure resulting from the displacement of fluid caused by the advancing blades, results in pressure variations in the air that it passes through, generating ”thickness noise” that adds to the BTI noise as the blades pass the tower.

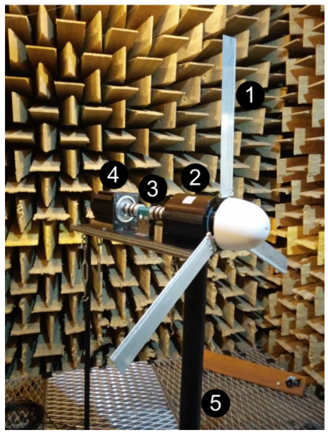

(a) Scale-model wind turbine

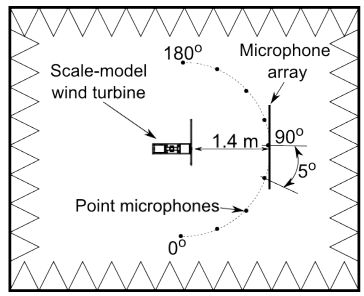

(b) Anechoic chamber measurement set-up

Fig. 3 Scale-model wind turbine. Parts are: (1) NACA 0012 airfoil (tripped at 10% chord length, 70 mm chord, 450 mm span), (2) Slip ring (24 channels), (3) Torque sensor, (4) AC driver and (5) Support tower (70 mm outer diameter)

The rotor model was driven at 900 RPM, giving a blade tip speed of ∼47 m/s and a blade-pass frequency of 45 Hz. The rotor plane was located 70 mm away from the closest point on the tower. This distance is comparable to one blade chord length and is found to be a good scaled representation of the blade-to-tower distance on a utility scaled wind turbine. The blade-tower interaction was investigated using point microphone measurements and a 1.5 m diameter circular microphone array containing 64 GRAS 40PH phase and magnitude matched microphones on a plane parallel to the rotor plane and 10 cm from it. The data obtained with the microphone array was processed using statistically optimised near-field acoustic holography (SONAH) (Hald, 2009) to obtain low-frequency sound source visualisation in the rotor plane.

Figure 4 shows the power spectral density of the blade-tower interaction noise measured on an axis perpendicular to the rotor plane centre. As can be seen, the spectrum consists of a series of “peaks” which are harmonically related to the blade-pass frequency of 45 Hz. It is also evident that the noise magnitude is inversely proportional to the distance *d* between the rotor plane and the support tower, which is in accordance with previous research (Madsen, 2010). This indicates that the support tower does have an effect on the blade loading via interaction with the potential field surrounding the blade and the noise production mechanism is identical to the one experienced by full-size wind turbines.

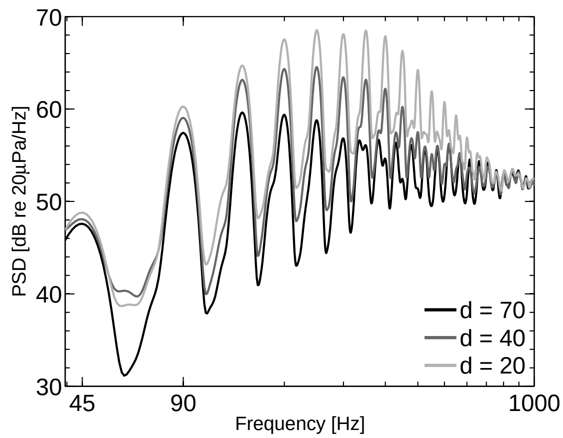

Fig. 4 Effect of the distance, d, between the support tower and the blade on the blade-tower interaction noise at 0° angle of attack

Figure 5 shows the directivity pattern for 45, 135, 360 and 450 Hz. These frequencies correspond to the 1st, 3rd, 8th and 10th harmonics of the blade-pass frequency, respectively. It can be seen that sound radiation at 135 Hz is omnidirectional, assuming symmetry across the rotor plane. For 360 and 450 Hz, a significant reduction in the sound pressure level is observed at angles $< 30°$ and $> 150°$. For 45 Hz, constructive interference is seen on each side of the rotor plane (between 0° and 30° and between 150° and180°) and destructive interference is seen at 60°. The constructive and destructive interference at any particular harmonic frequency is a result of the spinning mode acoustic interference in the rotor plane.

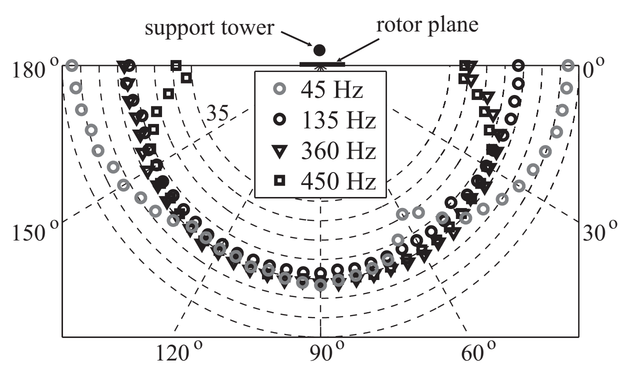

Fig. 5 Blade-tower interaction noise directivity pattern for selected frequencies. Dashed circular contours denote sound pressure level in dB and are 5dB apart

The SONAH sound field visualisation shown in Figure 6 indicates that the majority of energy at the blade-pass frequency, f = 45 Hz, in Fig. 6a originates at the support tower position. Radiation at higher blade-pass frequencies, f = 135, 360 and 450 Hz in Figs. 6b, 6c and 6d, respectively, is no longer highly concentrated at the support tower location but is rather spread out in the lower or middle part of the rotor plane. The most likely reason for the peak sound source being located slightly to the left of the tower in Fig. 6a, is that the peak loading occurs close to the leading edge (Wright, 1971). Since the blades are rotating in a clockwise direction, the leading edge is thus on the left side of the support tower when the blade is directly in front of the tower. The appearance of two sources in Fig. 6a, separated by the microphone spacing between the nine microphones in the outer circle of the array is an artefact of the SONAH process. This should be interpreted as a single source. Similarly the separate sources shown on the outer circle in 6b and 6c should be interpreted as a single source with intensity varying from a maximum at the bottom to a minimum at the top of the rotor plane.

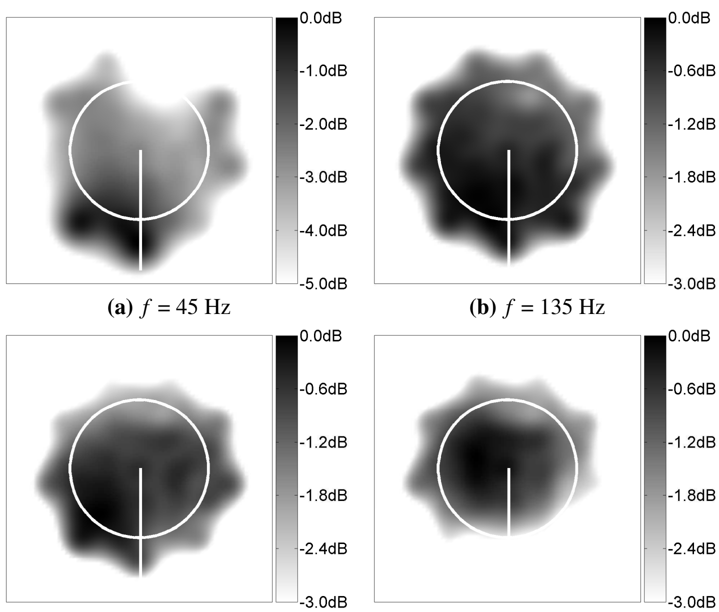

(**a**) f = 45 Hz (**b**) f = 135 Hz

(**c**) f = 360 Hz (**d**) f = 450 Hz

Fig. 6 Near-field acoustic holography. The white circle indicates the outer edge of the rotor plane and the thin white vertical line represents the support tower

The spread of the apparent source location at higher frequencies is an effect of the spinning modes and the frequency at which it begins to occur is a function of how close the observation plane is to the rotor plane.

6 Field measurements of propagation

Continuous indoor and outdoor measurements were carried out for periods of approximately one week at three residences located near the Waterloo wind farm, which is made up of 37 operational turbines. Outdoor measurements were made using a G.R.A.S. type 40AZ microphone with 26CG preamplifier with an electronic noise floor of 16 dB(A) and a low frequency linear response down to 0.5 Hz. Hemispherical secondary windshields of 450 mm diameter were used to minimise wind-induced noise, and they were designed to be consistent with the IEC-61400-11 (2012) standard. Wind speed and direction were measured at heights of 1.5 m and 10 m using Davis Vantage Vue and Vantage Pro weather stations, respectively. The weather measurements were collected in 5-minute intervals and then the 10-minute average was calculated during post-processing. Wind speed and direction at hub height were measured using a SODAR unit which was located on the ridge-top in the gap between the Northern and Southern wind turbine group shown in Fig. 7. The wind farm operator also provided hub height wind speed and direction for the period in which data for House 1 and House 2 were collected.

The location of the residences relative to the wind farm is shown in Fig. 7. House 1 is situated 3.5 km from the nearest wind turbine, which is near the centre of the main turbine group. The downwind direction from the closest wind turbine to the residence is 88°. House 2 is 8.7 km from the nearest wind turbine which is the northernmost turbine of the main group. The downwind direction from the closest wind turbine to the residence is 268°. House 3 is 3.3 km from the nearest wind turbine, which is the southernmost turbine in the smaller northern group. The downwind direction from the closest wind turbine to the residence is 300°. The wind speeds and directions at 1.5 m, 10 m and hub height are presented in Table 1 along with the overall power output of the wind farm and stability factor for the measurements shown in Fig. 7. For each measurement, the residence was located in a downwind direction (±45°) from the nearest wind turbine. It can be seen that the most stable conditions occurred during the measurements at House 3 according to the definition of stability factor, m.

$$m = \frac{\log_{10}\left(v_h/v_{ref}\right)}{\log_{10}\left(h/h_{ref}\right)} \tag{1}$$

where v_h is the velocity at 80 m hub height, v_{ref} is the velocity at 10 m, h is the height of wind turbine hub above a given residence and h_{ref} is 10 m.

Table 1 Wind and turbine operational conditions for the data shown in Fig. 8. Wind speed at hub height is for the turbine nearest to the residence

	Wind speed (m/s)			Wind direction (°)			Power	Stability
Description	1.5 m	10 m	hub height	1.5 m	10 m	hub height	Output (%)	factor
H1	1.8	3.4	10.5	135	135	133	44	0.4
H2	1.6	2.9	8.7	293	281	305	56	0.4
H3	0	0.4	10.4	-	22.5	287	53	1.1

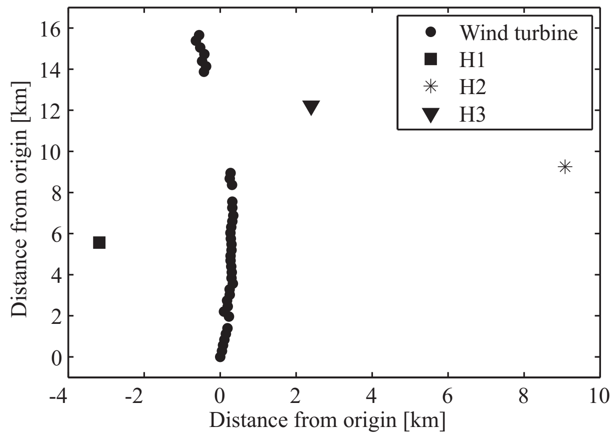

Fig. 7 Field measurement locations

Figure 8 shows the measured infrasound in the vicinity of the Waterloo wind farm at the three different locations. The harmonics of the blade-pass frequency of 0.8 Hz extend up to at least the 8^{th} order at all three residences, including the one located 8.7 km away from the wind farm. The relative amplitude of the peaks is consistent with their distances from the wind farm, and maximum attenuation occurs at H2. Propagation to H2 would also be affected by a ridge which is located between the residence and the wind farm and runs parallel to the line of wind turbines. The fundamental blade-pass frequency is not consistently visible in the outdoor spectra and this is attributed to the presence of wind-induced noise at some locations. The wind-induced noise raises the level of the broadband infrasound, particularly at very low frequencies and this causes masking of the peak at 0.8 Hz at H1 and H2. The blade-pass frequency harmonics can also be observed in the indoor results but the magnitude of the peaks below 6 Hz is not representative of the true signal due to the roll-off characteristic of the B&K 4955 microphones used for the indoor measurements.

Comparison between Figs. 4 and 8 indicates that there are striking similarities between the experimental and measured results. In both cases, the amplitude of the infrasonic peaks is significantly higher than the sound pressure levels at adjacent frequencies and the harmonics extend to similar orders. For the blade-tower spacing in Figure 4 of $d = 70$ mm, which represents the spacing for an industrial wind turbine based on scaling considerations, it can be seen that the relative amplitudes of the first six harmonics are similar to those in Figure 8, which were measured on an industrial turbine.

To investigate the effect of source height, receiver position and atmospheric velocity profile on the distance at which multiple reflections first occur, a ray tracing model was used and the results are shown in Fig. 9. Field measurement data published in a wide range of studies (Ljunggren (1996); Sondergaard and Plovsing

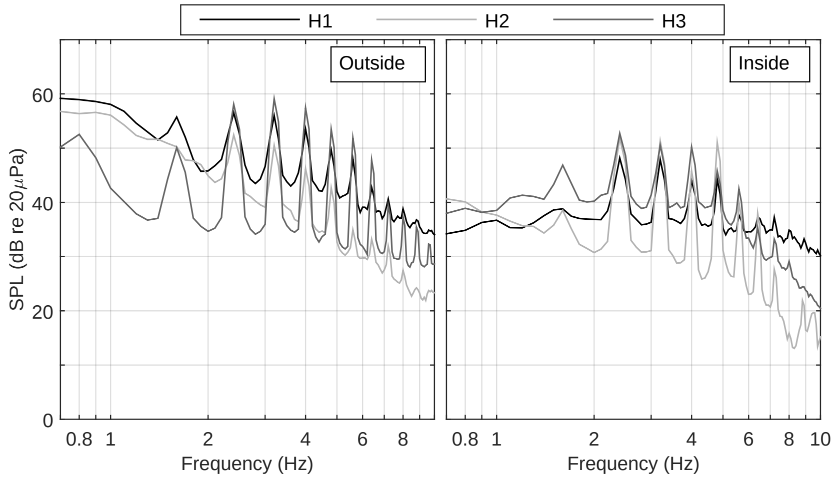

Fig. 8 Measured infrasound

(2005); Willshire Jr and Zorumski (1987); Boué (2007)) are also plotted for comparison. Differences between the model and measurements by others can be attributed to the vertical atmospheric sonic velocity profile associated with the measurements. Since this information was not available from the literature, the profile used in this study was specified according to SODAR data measured under stable atmospheric conditions (Hansen et al., 2015) and according to the logarithmic velocity profile used in the Nord2000 propagation model (Plovsing and Kragh (2006) and Plovsing (2007)). It is evident that the assumed vertical sonic velocity profile has a large impact on the model output, particularly at large propagation distances.

As indicated in Fig. 9, it is important to take into account the height of the source when considering propagation of noise from a wind farm. Since noise at infrasonic frequencies is attributed to blade-tower interaction, the source height for these frequencies is the point at which this interaction noise is maximum. In the case of the experiments presented in Sect. 5, the maximum noise occurred close to the blade-tip as the blade passed the tower. It is possible that this point would vary for an industrial wind turbine since the blades have significant twist and taper, which has a large impact on the corresponding aerodynamic forces. Nonetheless, it is anticipated that the source height for blade-tower interaction noise would be appreciably lower than the hub height, which is generally assumed as the relevant source height in propagation analyses. Therefore, the distance from the source at which multiple reflections first occur would be reduced. If the blade-tower interaction noise source is in fact located at the blade-tip for a Vestas V90 3MW wind turbine model (installed at Waterloo), the corresponding source height would be 36 m. According to Fig. 9, this would reduce the distance at which multiple reflections first arrive at the ground by 0.5 - 1.3 km, depending on the relevant velocity profile. Therefore, due to the contribution of an increased number of ray paths, the attenuation of noise at infrasonic

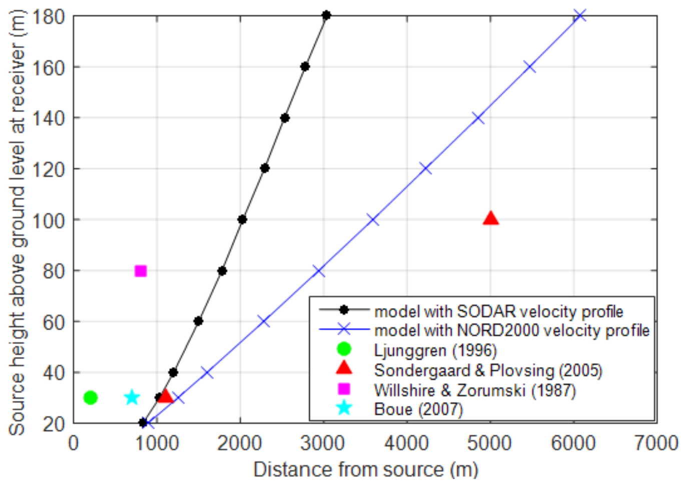

Fig. 9 Comparison between ray tracing results and published data for the distance from the source at which multiple ground reflections begin to occur

frequencies would be less than would be predicted if the source were assumed to be at hub height.

Determination of the relevant source height is also an important consideration for the other aerodynamic and mechanical noise sources that were discussed in Sect. 3. It is therefore important to determine the blade positions at which blade stall occurs, how mechanical noise is radiated by structural components such as the blades and tower and which blade location the noise due to inflow turbulence would be maximum. The directivity of these noise sources is also important.

7 Conclusions

Comparison between the field measured noise data near a wind farm and laboratory measurements using a motor-driven model turbine in zero incident flow reveals striking similarities in the infrasonic acoustic spectra. The accurate prediction of the propagation of this noise is dependent on the source height that is used, which is why the relative source height determined from laboratory measurements is a useful input to noise prediction models. The source height together with the vertical wind speed profile determine the distance from the source beyond which sound rays that have experienced more than one ground reflection will arrive at the receiver, thus resulting in increased noise levels over what would be expected due to a sound field decay of 6 dB per doubling of distance.

References

Boué, M. (2007). Long-range propagation over the sea with application to wind turbine noise. Technical report, KTH.

Doolan, C., Moreau, D. J., and Brooks, L. A. (2012). Wind turbine noise mechanisms and some concepts for its control. *Acoustics Australia*, 40(1):7–13.

Dooley, K. A. (2013). Significant infrasound levels a previously unrecognized contaminant in landmark motion sickness studies. *The Journal of the Acoustical Society of America*, 134(5):4097.

Dooley, K. A. and Metelka, A. (2014). Acoustic interaction as a primary cause of infrasonic spinning mode generation and propagation from wind turbines. volume 20, page 2272.

Hald, J. (2009). Basic theory and properties of statistically optimized near-field acoustical holography. *The Journal of the Acoustical Society of America*, 125(4):2105–2120.

Hansen, K., Hessler, G., Hansen, C., and Zajamsek, B. (2015). Prediction of infrasound and low frequency noise propagation for modern wind turbines: a proposed supplement to ISO 9613-2. In *Proceedings of WTN15, the sixth international conference on wind turbine noise*.

Hansen, K., Zajamsek, B., and Hansen, C. (2014). Comparison of the noise levels measured in the vicinity of a wind farm for shutdown and operational conditions. In *InterNoise 2014*.

IEC-61400-11 (2012). Wind turbine generator systems - part 11: acoustic noise measurement. Technical report, International standard IEC 61400-11.

Ljunggren, S. (1996). Ljudutbredning kring havsbaserade vindkraftverk. resultat fraan en litteraturstudie. Technical report, Department of Civil and Architectural Engineering, KTH.

Madsen, H. A. (2010). Low frequency noise from wind turbines mechanisms of generation and its modelling. *Journal of Low Frequency Noise, Vibration and Active Control*, 29(4):239–251.

Møller, H. and Pedersen, C. S. (2004). Hearing at low and infrasonic frequencies. *Noise and Health*, 6(23):37.

Møller, H. and Pedersen, C. S. (2011). Low-frequency noise from large wind turbines. *The Journal of the Acoustical Society of America*, 129:3727–3744.

Oerlemans, S. and Schepers, J. (2009). Prediction of wind turbine noise and validation against experiment. *International journal of aeroacoustics*, 8(6):555–584.

Plovsing, B. (2007). Proposal for nordtest method: Nord2000–prediction of outdoor sound propagation. *DELTA Acoustics, Report AV*, 1106(07).

Plovsing, B. and Kragh, J. (2006). Nord2000, comprehensive outdoor sound propagation model. part 2: Propagation in an atmosphere with refraction. *Delta Acoustics for Nordic Noise Group, Report AV 1851/00*.

RenewableUK (2013). Wind turbine amplitude modulation: research to improve understanding as to its cause & effect. Technical report.

Salt, A. N. and Lichtenhan, J. T. (2014). How does wind turbine noise affect people. *Acoust Today*, 10:20–28.

Sondergaard, B. and Plovsing, B. (2005). Noise from offshore wind turbines. *Environmental Project 1016*.

Tyler, J. M. and Sofrin, T. G. (1962). Axial flow compressor noise studies. *SAE Trans.*, 70:309.

Van den Berg, G. (2004). Effects of the wind profile at night on wind turbine sound. *Journal of Sound and Vibration*, 277:955–970.

Van den Berg, G. (2005). The beat is getting stronger: The effect of atmospheric stability on low frequency modulated sound of wind turbines. *Journal of Low Frequency Noise, Vibration and Active Control*, 24(1):1–24.

Willshire Jr, W. L. and Zorumski, W. E. (1987). Low-frequency acoustic propagation in high winds. In *NOISE-CON 87; Proceedings of the National Conference on Noise Control Engineering*, volume 1, pages 275–280.

Wright, S. (1971). Discrete radiation from rotating periodic sources. *Journal of Sound and Vibration*, 17(4):437–498.

Wright, S. (1976). The acoustic spectrum of axial flow machines. *Journal of Sound and Vibration*, 45(2):165–223.